Research Article

Received: 2 June 2021 Revised: 8 November 2021 Accepted article published: 17 November 2021 Published online in Wiley Online Library:

(wileyonlinelibrary.com) DOI 10.1002/pi.6331

Influence of CeO_2 as dispersoid in blend poly(styrene-*co*-methylmethacrylate) as electrolyte for lithium-ion battery

Murugesan Ramachandran,[a,b] Rengapillai Subadevi,[a] Palanisamy Rajkumar,[a] Rajendran Muthupradeepa[a,c] and Marimuthu Sivakumar[a*]

Abstract

Poly(styrene-*co*-methylmethacrylate) P(S-MMA) composite polymer electrolytes are having massive consideration for solid-state electrochemical devices. There are numerous tactics implement to improve the ambient temperature ionic conductivity such as the addition of plasticizers, the inclusion of nanosize ceramic fillers and blending with the host polymer, which were carried out in this work. The effect of CeO_2 on the P(S-MMA)-poly(vinylidene fluoride) (25:75 of 27 wt%)-$LiClO_4$ (8 wt %)-ethylene carbonate:propylene carbonate (1:1 of 65 wt%) system prepared via a conventional solution casting technique. The as-prepared polymer membranes were characterized using XRD, Fourier transform infrared spectroscopy, thermogravimetry and differential thermal analysis, SEM and AC impedance analyses. The composite polymer blend gel electrolyte system exhibits high ionic conductivity (2.51×10^{-2} S cm^{-1}) with 6 wt% CeO_2 nanofiller at ambient temperature. The conductivity enhancement is due to the presence of a rise in the amorphous content; it is in well concurrence with the XRD results. The optimum electrolyte was used to design the $LiFePO_4$/composite gel polymer electrolyte/Li cell couple in a 2032 type coin cell. It possesses a discharge capacity of 151 mA h g^{-1} at 0.1 C.

Supporting information may be found in the online version of this article.

Keywords: poly(styrene-*co*-methylmethacrylate); solution casting method; composite polymer electrolyte; blend polymer system

INTRODUCTION

Lithium-ion batteries (LIBs), which are widely used as power sources, have dominated the efficacy in portable devices, transportation and large-scale energy storage devices. The electrolyte is a noteworthy part of LIBs, where a volatile and flammable organic liquid is commonly used. Although it has a high ionic conductivity at room temperature, it creates problems such as corrosion of electrodes, leakage of liquid electrolyte and lithium dendrite evolution. Consequently, safety problems are the key challenges in the application of lithium polymer batteries.

Security risks can be significantly reduced if the organic liquid electrolytes have been substituted by durable and incombustible solid electrolytes.[1–3] The main issue with solid polymer electrolytes is the contact between the electrode and electrolyte, even if it has a small ionic conductivity at ambient temperature. Because of the small zigzag movement of the polymer chain combined with a lithium salt, blend polymer electrolytes enrich the ionic conductivity through simple compositional change. Most research has concentrated on gel polymer electrolytes (GPEs) because of their huge ionic conductivity at room temperature. Although the GPEs display larger ionic conductivity at room temperature, analogous to a liquid electrolyte, further characteristics such as mechanical strength, solvent retention ability and other aspects have also been enhanced for commercial applications. It is as good as other strategies to enhance the mechanical steadiness and ionic conductivity, when a very small amount of nanosized ceramic particles is dispersed in the polymer electrolyte.

CeO_2 has been recognized to be one of the best candidates to increase the ionic conductivity, owing to its high dielectric constant ($\varepsilon = 26$) and wide bandgap energy ($E_g = 5.5$ eV).[4] Tailoring the particle size of the CeO_2 nanofiller is an influential way to modify the functions of the fillers. Numerous studies have revealed that the tendency to increases the ionic conductivity by reducing the size of the inorganic filler at a certain concentration. However, the increase of ionic conductivity is not a single

* *Correspondence to: M Sivakumar, #120, Energy Material Laboratory, Department of Physics, Science Block, Alagappa University, Karaikudi 630 003, Tamil Nadu, India. E-mail: susiva73@yahoo.co.in*

a *#120, Energy Material Laboratory, Department of Physics, Science Block, Alagappa University, Karaikudi, India*

b *Department of Physics, Arumugam Pillai Seethai Ammal College, Tiruppattur, India*

c *Department of Physics, Sree Sastha Institute of Engineering and Technology, Chennai, India*

function with the filler size; other aspects, namely the interaction between the filler, polymer and spreading of cerium oxide units in the membrane structure, have an effect. The polymer dipole positioning is interrupted by the occurrence of CeO_2 fillers in the polymer membrane; this endorses flexible zigzag mobility as well as detachment of pairs of ions owing to the formation of charges in the ceramic filler surface.[5,6]

Mohamed Ali *et al.*[7] prepared the composition PEO (68)-PEG (16)-$LiClO_4$ (11)-EC (5)-CeO_2 (1) (PEO, poly(ethylene oxide); PEG, polyethylene glycol; EC, ethylene carbonate) with a conductivity of 1.18×10^{-4} S cm^{-1}. Yahata *et al.*[8] reported that nanosized silica particles were used as fillers in blend polymer electrolytes. Xiao *et al.*[9] used blend copolymer electrolytes with a better ionic conductivity (2.79×10^{-3} S cm^{-1}) at ambient temperature. Rajendran *et al.*[10] synthesized the PMMA-$LiClO_4$-Dimethaxypropane (DMP)-10 wt% CeO_2 system (PMMA, poly(methylmethacrylate); DMP, 2,2-dimethoxy-propane) with maximum conductivity 0.536×10^{-4} S cm^{-1} at 303 K. Ramachandran *et al.*[11] prepared a 6 wt% ZrO_2-P(S-MMA)-PVdF gel electrolyte system (P(S-MMA), poly(styrene-*co*-methylmethacrylate); PVdF, poly(vinylidene fluoride)) with discharge capacity 144 mA h g^{-1} at a rate of 0.1 C. Mahant *et al.*[12] synthesized a PMMA-PVdF based electrolyte with discharge capacity 140 mA h g^{-1} at a rate of 0.1 C after 50 cycles.

In GPEs, PVdF, PEO, PMMA, poly(vinyl chloride) (PVC) and polystyrene (PS) have commonly been used as a matrix. Among them, P(S-MMA) copolymer is a suitable matrix for LIB applications since the mechanical strength of GPEs may be developed by the styrene unit, owing to the low attraction of liquid electrolytes,[13] and PMMA acts as a gelatinization agent in the electrolyte and also has high anodic stability.[14] Numerous methods such as solution casting, plasticizer extraction, phase inversion, hot press and electrospinning techniques etc. have been extensively used for the synthesis of solid/gel polymers or nanocomposite polymer electrolytes. Among these, solution casting is a simple and most efficient technique to develop porous polymer electrolytes.[15–17]

Hitherto, the composition of P(S-MMA)-PVdF (25:75 of 27 wt %)-$LiClO_4$ (8)-EC + PC (65) polymer electrolytes (PC, propylene carbonate) was synthesized for lithium polymer battery application. The synthesized electrolytes were studied using XRD, Fourier transform infrared (FTIR) spectroscopy, AC impedance and SEM analyses. The optimized composition was used to fabricate a $LiFePO_4$/composite gel polymer electrolyte (CGPE)/Li based 2032 coin cell. Linear sweep voltammetry and cyclic voltammetry analyses were also carried out. The optimized electrolyte was used to determine the electrochemical performance such as charge/discharge analysis for the above-mentioned cell couple at 0.1 C.

Composite gel polymer blending is one of the most fashionable strategies with specific properties. CeO_2 nanoparticles with particle size 14 nm were synthesized by our group earlier.[18] In the present work, as-prepared CeO_2 nanofillers (particle size 14 nm) to 0, 3, 6, 9 and 12 wt% were spread into the augmented composition of P(S-MMA)-PVdF/$LiClO_4$ /EC + PC in the weight ratio 25–75 (27)/8/32.5 + 32.5) matrices. The solution casting technique was employed thorughout the process. The structural, thermal and AC impedance analyses are discussed here. The ionic conductivity is significantly improved (of the order of 10^{-2} S cm^{-1} with thermal stability at 280 °C) up to a concentration of 6 wt% CeO_2 as a solid plasticizer in the polymer matrix. The performance of LIB half-cells designed with the CGPE was inspected. As far as the authors are aware, no literature reports exist on the effect of CeO_2 particle size in the range below 20 nm on the transport properties of the above-mentioned polymer matrices. Therefore, it was important to study the impact of the nanosized inorganic filler CeO_2 film on the ionic conductivity and also the electrochemical properties of the CGPE.[19,20]

EXPERIMENTAL

PVdF (molecular weight 5.3×10^5); (Merck, Germany); P(S-MMA) (molecular weight 100–150); (Aldrich, Germany); $LiClO_4$ (Aldrich, Germany) and tetrahydrofuran (THF); (E-Merck, Germany)were utilized in the experiment. The solution casting technique was employed throughout the experiment. The stoichiometric amount of the above polymer and salt had been dried at the boiling point of water and liquefied in THF followed by the accumulation of plasticizers. The mixture was then agitated constantly until the solution became a uniform gelatinous liquid.

The synthesized CeO_2 (3, 6, 9 and 12 wt%) nanoparticles were spread in the polymer electrolytes. The ensuing mixture was transferred into a glass Petri dish and the THF was allowed to evaporate at room temperature. This method produced mechanically steady, discrete and malleable films with a width of 50–100 μm. The films were further dehydrated in a vacuum oven at a pressure of 10^{-3} Torr for 24 h at 60 °C to eliminate the THF. Structural analysis was accomplished on the prepared film using an XPERT-PRO instrument (Portugal) with Cu Kα radiation. FTIR characterization was carried out using a Thermo Nicolet 380 instrument (USA) in the range 4000–400 cm^{-1}. Conductivity measurements were studied in the frequency range between 40 Hz and 100 kHz using a Keithley 3300 LCZ meter (USA). The as-prepared samples were kept in the middle of two stainless steel electrodes which performed as the hindering terminal for the ions. The morphology of the prepared samples had been examined by SEM (Hitachi-S 4800, Germany). Thermogravimetry and differential thermal analysis (TG/DTA) was measured on a thermal analyzer (Shimadzu DTA-60AH, UK). The operation temperature was increased from 30 to 700 °C with an increasing heat rate of 10 °C min^{-1} under an air atmosphere.

A $LiFePO_4$/P(S-MMA)-PVdF-EC + PC-CeO_2/Li coin cell (CR-2032 type) with 6 wt% CeO_2 concentration was fabricated as described in our earlier paper.[21] The linear sweep voltammetry (LSV) and cyclic voltammetry (CV) tests were achieved using the BTS-55 Neware battery tester system (China) between potentials 2 and 4.5 V at ambient temperature at a scanning rate of 1 mV s^{-1}. The charge/discharge cycle was also carried out by using the BTS-55 Neware battery tester.

RESULTS AND DISCUSSION

An XRD study was employed to observe the structure of the polymer electrolytes. The XRD patterns of pure PVdF, pure P(S-MMA), $LiClO_4$, CeO_2, and P(S-MMA)-PVdF-EC + PC-CeO_2 (bare, 3, 6, 9, 12) wt%, named CB1, CB2, CB3, CB4 and CB5 respectively, are depicted in Fig. 1. The deflection peaks appearing at $2\theta = 28.46°$, 32.98°, 47.41° and 56.27° belong to the cubic structure of CeO_2 (JCPDS 81-0792). The addition of CeO_2 into the polymer electrolyte decreases the intensities of the characteristic peak of PVdF, predominantly the dominant peak at 2θ =20.8°. Figure 1 shows that as the CeO_2 concentration is increased up to 6 wt% (sample CB3) the crystallinity of the host polymer is decreased. The estimated degree of crystallinity is 0.036%. The rise in the amorphous nature causes a decrease in

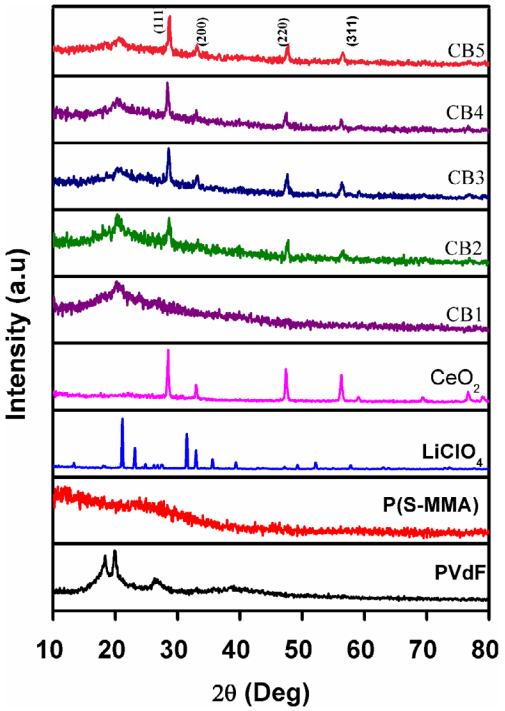

Figure 1. FTIR spectra of pure P(S-MMA), PVdF, $LiClO_4$, CeO_2 and P(S-MMA)-PVdF- $LiClO_4$-EC+PC polymer electrolytes with 0 (CB1), 3(CB2), 6 (CB3), 9(CB4) and 12(CB5) wt.% CeO_2.

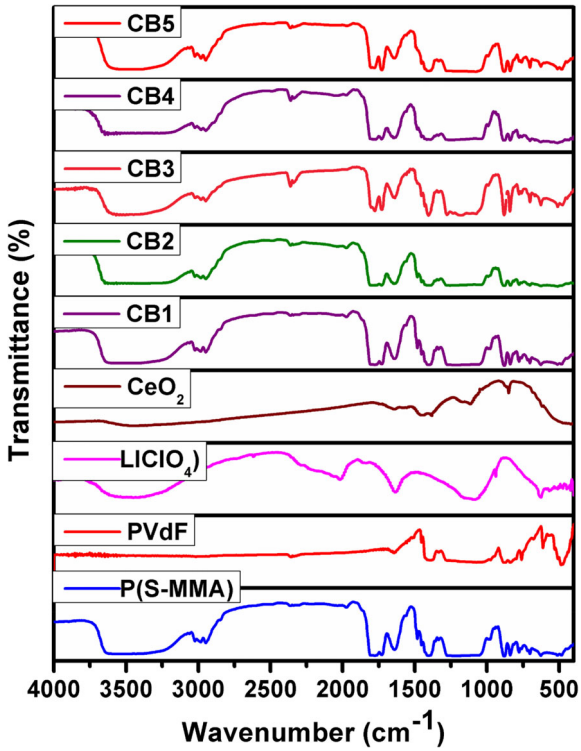

Figure 2. FTIR spectra of pure P(S-MMA), PVdF, $LiClO_4$ and CeO_2, and P(S-MMA)-PVdF-$LiClO_4$-EC + PC polymer electrolyte with 0 (CB1), 3 (CB2), 6 (CB3), 9 (CB4) and 12 (CB5) wt% CeO_2.

the energy barrier to the segmental motion of the polymer electrolytes, i.e. higher conductivity.[22,23] It has been observed that all peaks consistent with $LiClO_4$ are found to be absent in the complexes.

Infrared analysis is an influential instrument to recognize the bonding and different functional groups existing in the samples. The FTIR spectra of pure P(S-MMA), pure PVdF, pure $LiClO_4$, the as-prepared CeO_2 and the composite gel polymer blend electrolytes such as P(S-MMA)-PVdF-$LiClO_4$-CeO_2 (bare, 3, 6, 9 and 12 wt%) are shown in Fig. 2. The CH_2 scissoring mode of MMA appears at 1480 cm^{-1} and C–H stretching of a methyl group exists at 2900 cm^{-1} for pure P(S-MMA).[24] These bands are shifted to 1484, 1483, 1481, 1483 and 1493 cm^{-1} and 2941, 2946, 2948, 2947 and 2950 cm^{-1} respectively for all samples. The stretching vibration of C–O–C appears at 874 cm^{-1} and the carbonyl group of the C=O vibration has appeared at 1724 cm^{-1} in PMMA.[25] The bands are shifted to 883, 879, 881, 883 and 885 cm^{-1} and 1733, 1730, 1730, 1729 and 1731 cm^{-1}, respectively, in the as-prepared mixtures. The >C=O, >C=C< and CF bending vibrational peaks of PVdF appear at 1630, 1400 and 509 cm^{-1} respectively.[26] These bands are shifted to 1640, 1634, 1637, 1647 and 1645 cm^{-1}, 1406, 1415, 1407, 1418 and 1428 cm^{-1} and 513, 511, 509, 512 and 512 cm^{-1} respectively in all as-synthesized mixtures.

The significant EC band of $\gamma_{C=O}$ (skeletal breathing) seems to be at 1810 cm^{-1} because the Fermi resonance of skeletal breathing is lifted in the lesser wavenumbers of the mixtures, confirming complexation between EC and the polymer electrolyte.[27] The perchlorate anion for the $LiClO_4$ salt absorption band has been allocated at 940 cm^{-1}, which is lifted to 932 cm^{-1} in the complexes. The Ce–O stretching bands at 502 and 683 cm^{-1} are shifted to higher wavenumbers in all prepared complexes.[28] It is also found that some of the peaks, such as 1200 and 1833 cm^{-1}, disappeared in the complexes. Strange peaks are also noticed as 882 and 1403 cm^{-1}. The fluctuating absorption peaks, the addition of strange peaks and the absence of peaks reveal that complex formation has happened between the polymer and salt matrices.

SEM micrographs (magnification 5000×) of the prepared composite polymer blend gel electrolyte CGPE with CeO_2 (0, 3, 6, 9 and 12 wt%) are shown in Figs 3(a)–3(e). The images of bare CGPE (CB1) reveals that there are more voids in the matrix, while on adding CeO_2 filler into the polymer matrix the morphology is improved, utilizing more networks. It is found that dispersal of pores on the polymer electrolyte surface becomes thicker on gradually adding CeO_2 into the mixture reaches the maximum while the content of the CeO_2 is 6 wt%. Consequently, the increase in filler content causes a decrease in conductivity. In CGPE, the porous structure gives the conducting pathways of Li^+ mobility.[29,30] The external porous morphology of the prepared polymer electrolyte is efficiently designed due to the contact of the CeO_2 filler and the polymer module in addition to the associated fluid molecule.[31] Nevertheless, above 6 wt% of the CeO_2 nanofiller concentration to gel segment accumulated more on the P(S-MMA)-PVdF membrane and create the insulation of bunches. Meanwhile, all the films were prepared in the same environment, and modification of sponginess and variation of grains of the as-synthesized composition are anticipated to arise due to the varying CeO_2 composition. This phase aggregated insulation of percolation bunches hinders the ion mobility and therefore ionic conductivity. The SEM images imitate the ionic conductivity measurements. The SEM images (magnification 1000×) of the corresponding system are provided in the supporting information.

TG/DTA studies were performed in an air atmosphere to certify the thermal stability of the polymer electrolytes. The operation

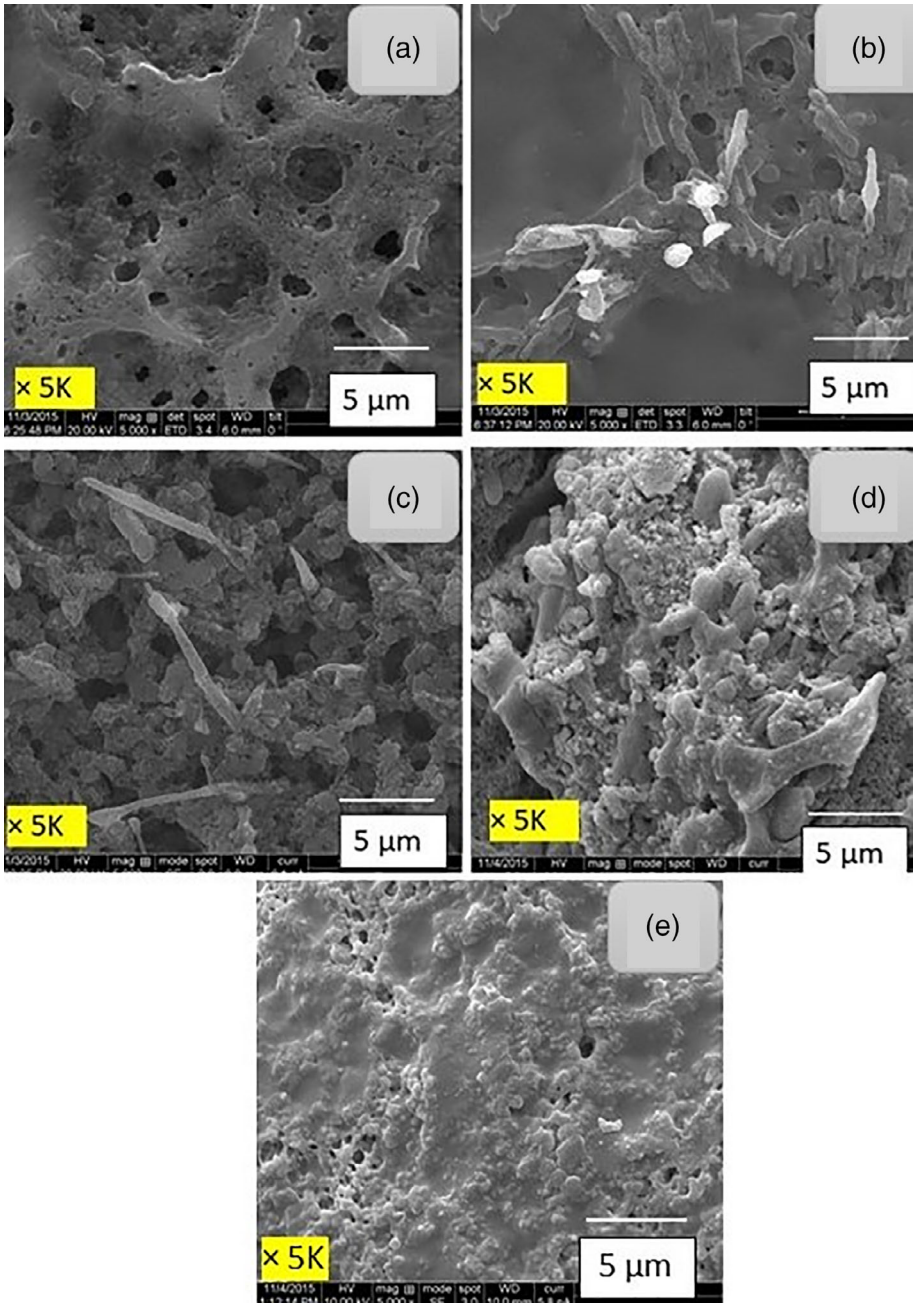

Figure 3. SEM images of (a) bare P(S-MMA)-PVdF-$LiClO_4$-EC + PC polymer electrolyte (CB1) with (b) 3 (CB2), (c) 6 (CB3), (d) 9 (CB4), (e) 12 (CB5) wt% CeO_2.

temperature was increased from 30 to 700 °C with an increasing heat rate of 10 °C min^{-1}. Figure 4 depicts the TG curve for P(S-MMA)-PVdF-$LiClO_4$-EC + PC-6 wt% CeO_2 electrolyte. It is observed from the TG curves that three weight losses correspond to the following temperatures: (i) 100 °C is associated with a weight loss of 10%, (ii) 280 °C is connected with a weight loss of 24% and (iii) 420–480 °C is linked with a weight loss of 35%. The first weight loss corresponds to expelling the solvent and moisture. The second weight loss corresponds to removal of the EC + PC mixture. The rapid third decline in weight is due to the decomposition of copolymer breaking bands like C–H, C–F etc. Finally, the residue was observed at 6 wt% in the TG curve. It is owing to the presence of inorganic filler in the complexes. It is also observed that the film containing 6 wt% CeO_2 mixture reveals maximum ionic conductivity and thermal stability up to 280 °C, which is more suitable for lithium battery application. Besides, the DTA curves of this sample validate a broad exothermic peak in the range 130–200 °C, which reveals the melting of the polymers (PVdF at 160 °C and P(S-MMA) at 200 °C).[32,33]

The optimized composite PBGE with 6 wt% CeO_2 is depicted in Fig. 5(a) at a temperature between 303 and 373 K. The conductivity is primarily due to the ions, because of the absence of a curved plot in the high frequency region of the complex impedance plot.[34,35] The parent electrolyte possesses an ionic conductivity of 3.1×10^{-4} S cm^{-1} at 303 K. When CeO_2 filler is incorporated into the parent electrolyte, the conductivity increases by one order of magnitude at 303 K. Also, it is shown that the inclusion of ceramic particles up to 6 wt% has increased the ionic

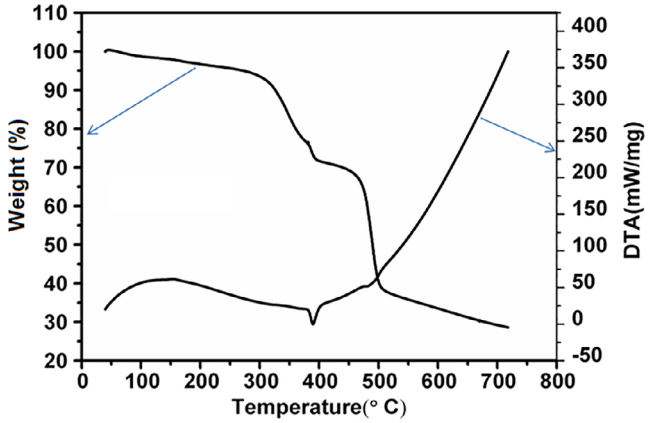

Figure 4. TG curve of P(S-MMA)-PVdF-$LiClO_4$-EC + PC-6 (CB3) wt% CeO_2 polymer electrolyte.

conductivity. The high ionic conductivity value of 2.52×10^{-2} S cm^{-1} at 302 K is reached for P(S-MMA)-PVdF (25:75 of 27 wt %)-$LiClO_4$ (8 wt%)-EC + PC (65 wt% of 1:1)-6 wt% CeO_2 among all the compositions studied. Further increase of filler content results in a decline in conductivity. This may be due to the spreading of nanosized particles, which powerfully impact the polymer chain, immobilizing it. Ceramic particles (6 wt%) act as a nucleation center for the formation of tiny crystallites and the creation of a new kinetic path via polymer–ceramic boundaries.[36] As already suggested by other groups,[37,38] O^{2-} and an OH^- surface group of filler interact with lithium ions over momentary hydrogen bonding, which makes extra leading pathways. According to the extensively recognized foundation mechanism of Composite polymer electrolyte (CPE), Lewis acid spots on the surface of the nanoparticles interrelate with the base center of ether oxygen in P(S-MMA)/PVdF chains in the creation of the composite. Furthermore, the filler interrelates with positive and negative ions and offers a supplementary large leading route in the neighborhood of CeO_2 particles for the movement of ions.[39,40] The addition of filler has supported the development of ionic conductivity by the following means: (i) the polymer segmental resistance could not alter abundantly, in fact, more flexible, (ii) the creation of additional hopping spots for lithium-ion migration and (iii) the increase in the amorphous stage of the transporting composition appears to be a probable mechanism triggered by the occurrence of CeO_2.[41]

Further, the addition of CeO_2 above 6 wt% causes a reduction in conductivity, which is due to ionic aggregation as well as ion pairs.[42] Table 1 shows that, as the temperature increases, the magnitudes of ionic conductivity also start to grow, which may be due to the volume expansion of the polymer matrix helping in free movements of ions.[43] The temperature dependence of the electrical conductivity (ln σ *versus* 1/*T*) for dissimilar configurations is displayed in Fig. 5(b). When the temperature rises, the conductivity also improves; this exposes that the polymer could be extended smoothly and formed the free volume. The subsequent conductivity is denoted by the motion of ions and polymer chains and is determined by the free volume around the polymer chain. It seems to obey the Vogel–Tamman–Fulcher model. This effect shows that the addition of fillers does not hinder the

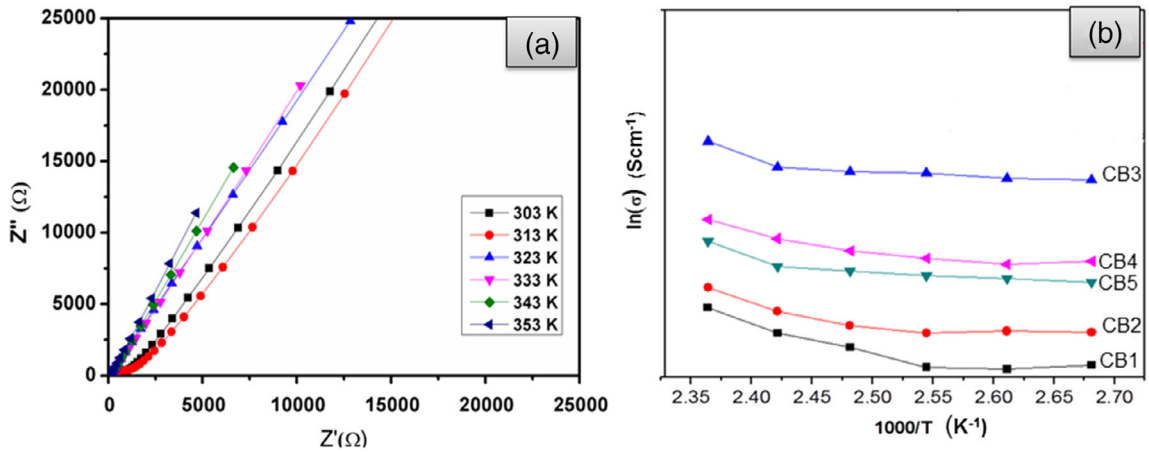

Figure 5. (a) Nyquist plot of P(S-MMA)-PVdF-$LiClO_4$-EC + PC-6 wt% CeO_2 polymer electrolyte. (b) Vogel–Tamman–Fulcher plots of P(S-MMA)-PVdF-$LiClO_4$-EC + PC-CeO_2 (bare, 3, 6, 9, 12 wt%) electrolytes.

Table 1. Ionic conductivity values of P(S-MMA)-PVdF-$LiClO_4$-EC + PC-CeO_2 (bare, 3, 6, 9 and 12 wt%) (CB1–CB5) in the temperature range 303–343 K

		Conductivity $\times 10^{-3}$ S cm^{-1}					
Sample	CeO_2 (wt%)	303 K	313 K	323 K	333 K	343 K	E_a values (eV)
CB1	0	0.31	0.34	0.46	0.59	0.63	0.34
CB2	3	1.6	1.68	1.72	1.79	1.84	0.24
CB3	6	25.2	26.1	26.8	27.4	27.9	0.14
CB4	9	8.12	8.71	9.42	9.95	10.21	0.18
CB5	12	6.21	6.81	7.07	7.97	8.15	0.21

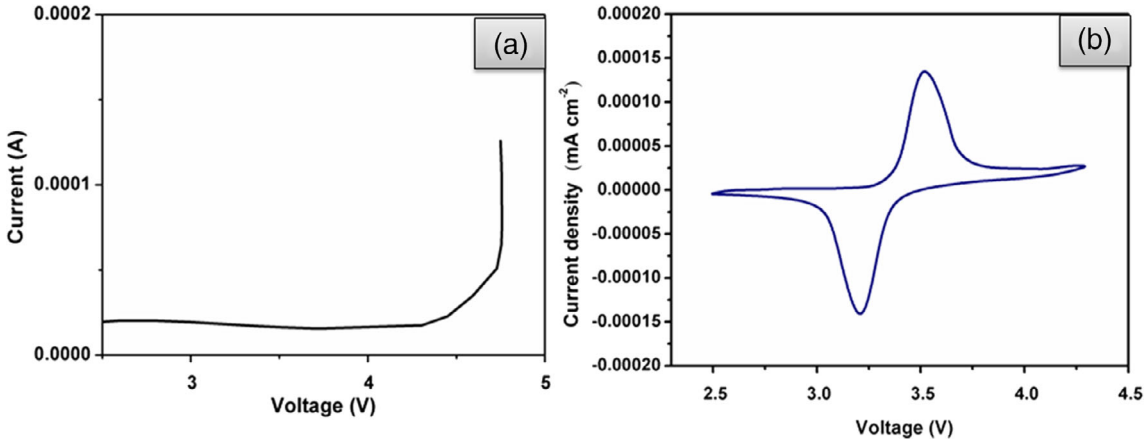

Figure 6. (a) Linear sweep and (b) cyclic voltammogram of the $LiFePO_4$/CB3/Li cell.

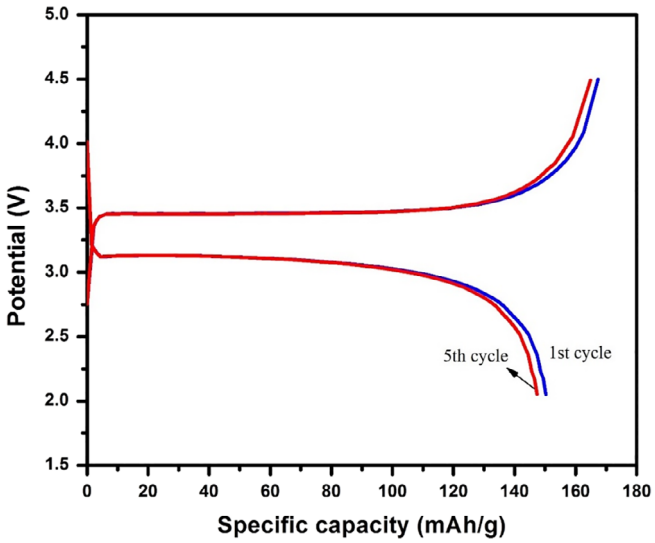

Figure 7. Charge–discharge profile for Li/CB3/$LiFePO_4$ at 303 K; cut-off voltage 2–4.5 V.

movement of lithium ions in the polymer matrix. It is also inferred that high ionic conductivity is detected for the 6 wt% CeO_2 based polymer electrolyte system; the reduced size of CeO_2 gives this composite PBGE enhanced conductivity. Also, this result is higher than the value reported in the literature[44,45] for the PVdF-*co*-hexafluoropropylene (HFP) based system and the PVC-CeO_2-dibutyl phthalate (DBP)system. This may be due to the minimal size and higher dielectric constant of CeO_2 and also its high electronegativity. Furthermore, the activation energy is calculated using the Arrhenius equation $\sigma = \sigma_0 \exp(-E_a/kT)$. Here σ is the ionic conductivity of the sample, σ_0 is the pre-exponential factor, E_a is the activation energy, k is Boltzmann's constant and T is the absolute temperature. We plot the graph of $1000/T$ against log σ and take the slope of the curve (Fig. 5(b)) to find the activation energy.

Linear sweep voltammetry covered the electrochemical steadiness range of the prepared polymer matrix and the voltammogram is illustrated in the Fig. 6(a). There is no noticeable electron flow through the sensitive terminal from 2 to 4.6 V and then electron flow associated with the disintegration of the transporting path is progressively improved at 4.7 V, which indicates the improvement of the oxidative stability of the CGPE. The current response graph dictated that the enhancement can be ascribed to the stability of the electrolyte components. Figure 6(b) illustrates the cyclic voltammograms of the prepared CB3 electrolyte based cell at a scan rate of 1 mV s^{-1} at room temperature with a voltage range of 2.5–4.3 V. From the cyclic voltammetry curve, the redox peaks at *ca* 3.2 and *ca* 3.5 V *versus* Li/Li^+ represent the reduction and oxidation curves, respectively; this confirms the deinsertion/insertion of Li^+ ions in the electrolyte. The presence of intercalation and de-intercalation peaks suggests a strong reversible performance of the prepared electrolyte material. The oxidation peak resembles the disintegration process of the electrolyte, causing the creation of a solid electrolyte interface film on the exterior of the terminal, and the reduction peak corresponds to lithium deposition.[46]

Figure 7 depicts the typical galvanostatic discharge/charge profile of the fabricated CB3 electrolyte based sample at 0.1 C rate at room temperature with a cut-off voltage of 2– 4.3 V. The initial charge and discharge capacities are 167 and 150 mA h g^{-1} with a coulombic efficacy of 89.8%. The prepared sample achieves 88% of the theoretical value, thus indicating that the $LiFePO_4$ created in this work has good kinetics and that it can efficiently function in a battery having a polymer electrolyte.[47] In the fifth cycle, the cell brings an alterable capacity of 147 mA h g^{-1} with capacity maintenance of 98% being attained. These results confirm that the prepared polymer electrolyte effectively enhances the performance of the LIB.

CONCLUSION

CeO_2 nanoparticles (0, 3, 6, 9 and 12 wt%) dispersed in P(S-MMA)-PVdF based PBGE were synthesized using a solution casting technique. The complex formation was established by FTIR and XRD analyses. The 6 wt% CeO_2 based P(S-MMA)-PVdF (25:75 of 27 wt %)-$LiClO_4$ (8)-EC + PC (65) electrolyte exhibited the highest ionic conductivity of 2.51×10^{-2} S cm^{-1}. The temperature-dependent ionic conductivity values obeyed Vogel–Tamman–Fulcher behavior. The high ionic conductivity and the discharge capacity (151 mAh g^{-1}) for 6 wt% of CeO_2 based CGPE are attained, owing to its high electronegativity, high dielectric constant and lesser particle size (14 nm). The prepared film was thermally stable up to 280 °C. From the above studies, it can be assumed that the optimized nanocomposite PBGE system can be used for potential electrolytes in lithium polymer batteries.

ACKNOWLEDGEMENTS

One of the authors, M. Sivakumar, gratefully acknowledges UGC-New Delhi financial support under UGC-MRP F.No. 41-839/2012. All authors from Alagappa University acknowledge the financial support by DST-SERB, New Delhi, under the physical sciences grant sanctioned vide EMR/2016/006302. Also, all the authors gratefully acknowledge extension of the analytical facilities in the Department of Physics, Alagappa University, under the PURSE program, sponsored by the Department of Science and Technology (DST), New Delhi, Government of India, and the Ministry of Human Resource Development RUSA-Phase 2.0 grant sanctioned vide Lt.No. F-24-51/2014 U Policy (TNMulti Gen), Depertment of Education, Government of India.

SUPPORTING INFORMATION

Supporting information may be found in the online version of this article.

REFERENCES

1 Han F, Westover AS, Yue J, Fan X, Wang F, Chi M *et al*., *Nat Energy* **4**: 187–196 (2019).
2 Pozin M and Wicelinski S, Chapter 4 - Fundamentals, Systems and Applications Li-Battery SafetyElectrochemical power sources: fundamentals, systems, and applications, in *Li-Battery Safety*. Elsevier Pub, Cambridge, MA02139, United states, pp. 83–111 (2019).
3 Kobayashi Y, Shono K, Kobayashi T, Ohno Y, Tabuchi M, Oka Y *et al*., *J Power Sources* **341**:257–263 (2017).
4 Phoka S, Laokul P, Swatsitang E, Promarak V, Seraphin S and Maensiri S, *Mater Chem Phys* **115**:423–428 (2009).
5 Wu J, Zuo X, Chen Q, Deng X, Liang H, Zhu T *et al*., *Electrochim Acta* **320**: 134567 (1-11) (2019).
6 Naveen Kumar K, Saijyothi K, Kang M, Ratnakaram YC, Hari KK, Jin D *et al*. *Appl Phys A* **122**:1–14 (2016).
7 Mohamed Ali T, Padmanathan N, Selladurai S, *Ionics* **21**:829–840 (2015).
8 Yahata Y, Kimura K, Nakanishi Y, Marukane S, Sato T, Tsujii Y *et al*., *Langmuir* **35**:3733–3747 (2019).
9 Xiao Q, Wang X, Li W, Li Z, Zhang T, Zhang H, *Membr Sci* **334**:117–122 (2009).
10 Rajendran S, Mahendran O, Kannan R, *J Phys Chem Solid* **63**:303–307 (2002).
11 Ramachandran M, Subadevi R, Rajkumar P, Muthupradeepa R and Sivakumar M, *JApplPolymSci* **138**:51180 (2021).
12 Mahant YP, Kondawar SB, Nandanwar DV, Koinkar P, *Mater Renew Sustain Energy* **7**:5 (2018).
13 Kang D-W, Kim D-W, Jo S-I and Sohn H-J, *J Power Sources* **112**:1–7 (2002).
14 Takano T, Mikazuki A, Kobayashi T, *Polym Eng Sci* **54**:78–84 (2014).
15 Habiba U, Shariul Islam M, Siddique TA, Afifi AM, Ang BC, *Carbohy. Polym* **149**:317–331 (2016).
16 Verma A, Budiyal L, Sanjay MR, Siengchin S, *Polym Eng Sci* **59**:2041–2051 (2019).
17 Wang Y, Xiong S, Wang X, Chu J, Zhang R, Wu B *et al*., *PolymEngSci* **60**: 2204–2213 (2020).
18 Ramachandran M, Subadevi R and Sivakumar M, *Vacuum* **161**:220–224 (2019).
19 Raut P, Li S, Chen YM, Zh Y and Jana SC, *ACS Omega* **4**:18203–18209 (2019).
20 Zhan Z, Jana SC, *SPE Polymers* **1**:55–65 (2020).
21 Muruganantham R, Sivakumar M, Subadevi R, *J Power Sources* **300**: 496–506 (2015).
22 Kamada K, Sakagami Y, Mizokuro T, Fujiwara Y, Kobayashi K, Hirata S *et al*., *Mater Horiz* **4**:83–87 (2017).
23 Angulakshmi N, Thomas S, Naham KS, Manuel Stephan A, Nimma Elizabeth R, *Ionics* **17**:407–414 (2011).
24 Li W, Xing Y, Wu Y, Wang J, Chen L, Yang G *et al*., *Electrochim Acta* **151**: 289–296 (2015).
25 Abdus Subhan MD, Ahmed T, *Spectrochim Acta A* **129**:377–381 (2014).
26 Rajendran S, Sivakumar M, Subadevi R, *Mater Lett* **58**:641–649 (2004).
27 Croce F, Appetecchi GB, Persi L, Scrosati B, *Nature* **394**:456–458 (1998).
28 Deka M, Nath AK, Kumar A, *J Membr Sci* **327**:188–194 (2009).
29 Aravindan V and Vickraman P, *Euro Polym J* **43**:5121–5127 (2007).
30 Xue J, Xie J, Liu W and Xia Y, *Acc Chem Res* **50**:1976–1987 (2017).
31 Baskaran R, Selvasekarapandian S, Kuwat N, Kawamur J and Hattori TDSC, *MaterChem Phy* **98**:55–61 (2006).
32 Ortega PFR, Trigueiro JPC, Silva GG, Lavall RL, *Electrochim Acta* **188**: 809–817 (2016).
33 Mejia A, Devaraj S, Guzman J, Miguel Lopezdel Amo J, Garcia N, Rojo T *et al*., *J Power Sources* **306**:772–778 (2016).
34 Liang B, Jiang Q, Tang S, Li S, Chen X, *J Power Sources* **307**:320–328 (2016).
35 Croce F, Settimi L and Scrosati B, *Electrochem Commun* **8**:364–368 (2006).
36 Zhu Y, Wang Liu L, Xiao S, Chang Z, Wu Y, *Energ Environ Sci* **6**:871–878 (2013).
37 Fu X, Yu D, Zhou J, Li S, Gao X, Han Y *et al*., *Cryst Eng Comm* **18**:4236–4258 (2016).
38 Lim HR, Kim HS, Qazi R, Kwon YT, Jeong JW and Yeo WH, *AdvMater* **32**: 1901924 (2020).
39 Abhilash KP, Selvin PC, Nalini B, Jose R, Hui X, Elim HI *et al*. *Solid State Ion*. **341**:115032 (2019).
40 Jaipal Reddy M, Siva Kumar J, Subba Rao UV, Chu PP, *Solid State Ionics* **177**:253–256 (2006).
41 Long L, Wang S, Xiao M and Meng YJ, *JMaterChemA* **4**:10038–10069 (2016).
42 Masoud EM, El-Bellihi A-A, Bayoumy WA, Mohamed EA, *J Mol Liq* **260**: 237–244 (2018).
43 Ma Y, Li LB, Gao GX, Yang XY, You Y, *Electrochim Acta* **187**:535–542 (2016).
44 Arya A, Sharma AL, *Ionics* **23**:497–540 (2017).
45 Manuel Stephan A, *EuroPolymJ* **42**:21–42 (2006).
46 Osman Z, Arof AK, *Electrochim Acta* **48** (8):993–999 (2003).
47 Zagorski J, Silvan B, Saurel D, Aguesse F and Llordes A, *ACS Appl Energy Mater* **3**:8344–8355 (2020).

